

Commun. Theor. Phys. **75** (2023) 045701 (8pp) https://doi.org/10.1088/1572-9494/acbd94

Non-Hermitian Ising model at finite temperature

Qian Du, Kui Cao and Su-Peng Kou*

Center for Advanced Quantum Studies, Department of Physics, Beijing Normal University, Beijing 100875, China

E-mail: spkou@bnu.edu.cn

Received 23 November 2022, revised 18 February 2023
Accepted for publication 21 February 2023
Published 12 April 2023

Abstract

As a very simple model, the Ising model plays an important role in statistical physics. In the paper, with the help of quantum Liouvillian statistical theory, we study the one-dimensional non-Hermitian Ising model at finite temperature and give its analytical solutions. We find that the non-Hermitian Ising model shows quite different properties from those of its Hermitian counterpart. For example, the 'pseudo-phase transition' is explored between the 'topological' phase and the 'non-topological' phase, at which the Liouvillian energy gap is closed rather than the usual energy gap. In particular, we point out that the one-dimensional non-Hermitian Ising model at finite temperature can be equivalent to an effective anisotropic XY model in the transverse field. This work will help people understand quantum statistical properties of non-Hermitian systems at finite temperatures.

Keywords: non-Hermitian quantum system, Ising model, quantum statistical mechanics, thermodynamics

(Some figures may appear in colour only in the online journal)

1. Introduction

The Ising model is one of the simplest models in statistical physics [1, 2]. For the one-dimensional Ising model, the ground state is either a ferromagnetic order or an antiferromagnetic one [3]. At finite temperatures, due to thermal fluctuations, the long-range order disappears. When considering the transverse external field, we have a transverse Ising model [4–8]. Now, quantum phase transition caused by quantum fluctuations occurs between the long-range order and the spin-polarized state [9–12]. Near the quantum critical point, it manifests as a nonanalytical behavior in the ground state energy of the system. These greatly impact the understanding of the thermodynamic and dynamic properties of many condensed-matter systems.

At the same time, in recent years, the emergence of non-Hermitian physics has opened up a new direction for the study of physics. It refers to that the Dirac Hermitian conjugation of the Hamiltonian in the non-Hermitian systems is not itself [13]. This differs from the Hermitian system which has the conservation of probability and the real-valuedness of the expected value of energy versus a quantum state. In contrast, its probability is non-conservative due to the loss of energy and particles and information to external environments and the expected value of energy versus a quantum state is complex [14]. These characteristics lead to non-Hermitian systems exhibiting a great deal of astonishing physical phenomena, such as biorthogonality of eigenstates [15], exceptional points [16, 17], parity-time symmetry [18, 19], and pseudo-Hermiticity [20, 21]. As a result, significant progress in non-Hermitian quantum systems has been made in theoretical and experimental aspects [22–33], including non-Bloch bulk-boundary correspondence [34–40] and non-Hermitian skin effect [41–43]. However, the properties of non-Hermitian quantum systems at finite temperatures have not been fully investigated so far.

In the paper, we explore the physical properties of the one-dimensional non-Hermitian Ising model at finite temperature according to the quantum Liouvillian statistical theory. Based on the Liouvillian Hamiltonian of the system, we find that there exists a 'pseudo-phase transition' between the 'topological' phase and the 'non-topological' phase, which is accompanied by the Liouvillian energy gap closed rather than the usual energy gap closed. In addition, we point out that the one-dimensional non-Hermitian Ising model at finite temperature

* Author to whom any correspondence should be addressed.

can be equivalent to an effective anisotropic XY model in the transverse field. For the case of a strong non-Hermitian strength limit, the system becomes an effective isotropic XY model in the transverse field. In the high-temperature limit, the system appears the non-thermalization, which is different from the Hermitian system. This work can provide a reference for the study of non-Hermitian systems at finite temperatures.

The outline of this paper is as follows: In section 2, we show the quantum Liouvillian statistical theory for non-Hermitian quantum systems at finite temperatures. In section 3, we study the one-dimensional non-Hermitian Ising model at finite temperature and give its analytical solutions. For its Liouvillian Hamiltonian, the 'pseudo-phase transition' is explored between the 'topological' phase and the 'non-topological' phase. Furthermore, we find the one-dimensional non-Hermitian Ising model at finite temperature can be equivalent to an effective anisotropic XY model in the transverse field. In this model, we discuss its thermodynamic properties in Hermitian and non-Hermitian cases, and in the zero-temperature and high-temperature limits, respectively. In section 4, we draw the conclusion.

2. Quantum Liouvillian statistical theory

To study the properties of non-Hermitian systems at finite temperatures, the quantum Liouvillian statistical theory introduces the definition of the non-Hermitian thermal state. It indicates that a non-Hermitian system at finite temperature can evolve over time from any initial state to a unique state, which is called a non-Hermitian thermal state [44]. Such a non-Hermitian thermal state dominates the physical properties of the system.

For non-Hermitian systems in which the eigenvalues of its non-Hermitian Hamiltonian $\hat{H}_{\rm NH}$ are all real, people always call it a quasi-Hermitian system. For the quasi-Hermitian system, the density matrix in the non-Hermitian thermal state is [44]

$$\rho^{S}_{\rm NHTS} = \hat{S}\rho_0\hat{S}^{\dagger}, \tag{1}$$

where $\hat{S}$ is a similar transformation which can transform non-Hermitian Hamiltonian $\hat{H}_{\rm NH}$ into the Hermitian Hamiltonian $\hat{H}_0$ by

$$\hat{H}_0 = \hat{S}^{-1}\hat{H}_{\rm NH}\hat{S}.$$

The energy levels E_n of $\hat{H}_{\rm NH}$ (or $\hat{H}^{\dagger}_{\rm NH}$) are the same as those of $\hat{H}_0$. $\rho_0 = {\rm e}^{-\beta_T\hat{H}_0}$ is the density matrix of the Hermitian model $\hat{H}_0$ at the thermodynamic equilibrium, where β_T is the inverse temperature. As a result of $\hat{S}\rho_0\hat{S}^{\dagger} = {\rm e}^{-\beta_T\hat{H}_L}$, this type of non-Hermitian system at finite temperature can be expressed by the Liouvillian Hamiltonian $\hat{H}_L$

$$\hat{H}_L = -\frac{1}{\beta_T}\ln[\hat{S}({\rm e}^{-\beta_T\hat{H}_0})\hat{S}^{\dagger}]. \tag{2}$$

Its corresponding eigenvalue E^L_n and eigenstate are the Liouvillian energy level and Liouvillian state, respectively. It should be pointed out that $\hat{H}_L = \hat{H}^{\dagger}_L$ and E^L_n must be real.

In particular, there is non-thermalization at high temperature. Because when the temperature is high, $\beta_T \to 0$, the density matrix $\rho^{S}_{\rm NHTS}$ for a non-Hermitian system with all real spectra at the non-Hermitian thermal state is reduced to

$$\rho^{S}_{\rm NHTS} \sim \hat{S}\hat{S}^{\dagger} \neq \hat{I}. \tag{3}$$

As a result, the weights of microscopic quantum states are not the same and the system is not thermalized. This is very different from that of the usual Hermitian model, in which the density matrix at the thermodynamic equilibrium in high temperature is ${\rm e}^{-\beta_T\hat{H}_0} \sim \hat{I}$. This means the weights of all microscopic quantum states of the Hermitian systems are the same and the system exists the thermalization effect.

3. One-dimensional non-Hermitian Ising model in the transverse field

According to the above theory, we calculate the Liouvillian Hamiltonian of the one-dimensional non-Hermitian Ising model at finite temperature in the case of all real eigenvalues of the non-Hermitian Hamiltonian. Followed by it, we study its 'topological' properties and thermodynamic characteristics in detail.

3.1. The Jordan–Wigner transformation and the Liouvillian Hamiltonian

We consider a one-dimensional non-Hermitian Ising model, in which its Hamiltonian $\hat{H}_{\rm NHIS}$ can be written as [45]

$$\hat{H}_{\rm NHIS} = -J\sum_{j}^{N}\sigma_j^{x,\beta_{\rm NH}}\sigma_{j+1}^{x,\beta_{\rm NH}}, \tag{4}$$

where

$$\sigma_j^{x,\beta_{\rm NH}} = \hat{S}\sigma^x\hat{S}^{-1} = \cosh(\beta_{\rm NH})\cdot\sigma_j^x + {\rm i}\sinh(\beta_{\rm NH})\cdot\sigma_j^y. \tag{5}$$

$J>0$ is the coupling between the neighboring spins. This model can be transformed into the Hermitian Ising model

$$\hat{H}_0 = -J\sum_{j}^{N}\sigma_j^x\sigma_{j+1}^x, \tag{6}$$

under the similar transformation $\hat{S} = {\rm e}^{\beta_{\rm NH}\hat{H}'}$, where $\hat{H}' = \frac{1}{2}\sum_j\sigma_j^z$ and $\beta_{\rm NH}$ denotes the non-Hermitian strength. Due to the non-Hermitian similarity, the energy levels for $\hat{H}_{\rm NHIS}$ and $\hat{H}_0$ are the same. In this paper, we set $J=1$.

It is well known that the one-dimensional Hermitian Ising model can be mapped to the superconducting states by the Jordan–Wigner transformation to explore the corresponding many-body physics. For the Hermitian model $\hat{H}_0 = -J\sum_j^N\sigma_j^x\sigma_{j+1}^x$, the Jordan–Wigner transformation is defined by the string-like creation and annihilation operators

$$c_j^{\dagger} = \sigma_j^{\dagger}\prod_{l<j}(-\sigma_l^z), \quad c_j = \prod_{l<j}(-\sigma_l^z)\sigma_j^-. \tag{7}$$

So the fermion number operator becomes

$$\hat{n}_j = c_j^{\dagger}c_j = \frac{1}{2}(1+\sigma_j^z). \tag{8}$$

Under Jordan–Wigner transformation, the one-dimensional Hermitian Ising model becomes a one-dimensional Kitaev model with an imbalanced p-wave superconductor paring [46–48]

$$\hat{H}_0 = -J\sum_{j=1}^{N}(c_j^\dagger c_{j+1} + c_{j+1}^\dagger c_j + c_j^\dagger c_{j+1}^\dagger + c_{j+1}c_j). \tag{9}$$

Based on the Fourier transform $c_j = \frac{1}{\sqrt{N}}\sum_k c_k e^{ikR_j}$ and $c_j^\dagger = \frac{1}{\sqrt{N}}\sum_k c_k^\dagger e^{-ikR_j}$, we can rewrite the fermion Hamiltonian $\hat{H}_0$ as

$$\hat{H}_0 = \sum_{k>0}\psi_k^\dagger \hat{h}_0(k)\psi_k, \tag{10}$$

in momentum space by introducing $\psi_k = \begin{pmatrix} c_k \\ c_{-k}^\dagger \end{pmatrix}$ and $\psi_k^\dagger = \begin{pmatrix} c_k^\dagger & c_{-k} \end{pmatrix}$, where

$$\hat{h}_0(k) = 2J(-\cos k\cdot\tau^z + \sin k\cdot\tau^y), \tag{11}$$

and $\tau^{y,z}$ are the Pauli matrices. Here, we assume that N is even. $k = 0, \pm\frac{2}{N}\pi, \cdots, \pm\frac{N-2}{N}\pi, \pi$ for $c_{j+N} = c_j$ and $k = \pm\frac{1}{N}\pi, \pm\frac{3}{N}\pi\cdots, \pm\frac{N-1}{N}\pi$ for $c_{j+N} = -c_j$. The dispersion of the quasiparticle is given by

$$E_0(k) = \pm 2J. \tag{12}$$

Moreover, we have

$$\hat{H}' = \frac{1}{2}\sum_j \sigma_j^z \to \hat{H}' = \frac{1}{2}\sum_k \psi_k^\dagger \tau^z \psi_k. \tag{13}$$

For the non-Hermitian model, the Jordan–Wigner transformation turns into

$$\begin{aligned} \tilde{c}_j^\dagger &= \hat{S}\sigma_j^\dagger \prod_{l<j}(-\sigma_l^z)\hat{S}^{-1} = e^{\beta_{NH}}c_j^\dagger, \\ \tilde{c}_j &= \hat{S}\prod_{l<j}(-\sigma_l^z)\sigma_j^-\hat{S}^{-1} = e^{-\beta_{NH}}c_j. \end{aligned} \tag{14}$$

Then one-dimensional non-Hermitian Ising model is transformed into the one-dimensional non-Hermitian Kitaev model

$$\begin{aligned} \hat{H}_{NHK} = -J\sum_{j=1}^{N}(&c_j^\dagger c_{j+1} + c_{j+1}^\dagger c_j \\ &+ e^{2\beta_{NH}}c_j^\dagger c_{j+1}^\dagger + e^{-2\beta_{NH}}c_{j+1}c_j). \end{aligned} \tag{15}$$

Finally, under the periodic boundary condition, the non-Hermitian Hamiltonian of the one-dimensional non-Hermitian Ising model in momentum space is

$$\hat{H}_{NHK}(k) = \sum_{k>0}\psi_k^\dagger \hat{h}_{NHK}(k)\psi_k, \tag{16}$$

where

$$\hat{h}_{NHK}(k) = 2J(\sin k\cdot\tau^{y,\beta_{NH}} - \cos k\cdot\tau^z), \tag{17}$$

with

$$\tau_j^{y,\beta_{NH}} = \cosh(2\beta_{NH})\cdot\tau_j^y - i\sinh(2\beta_{NH})\cdot\tau_j^x. \tag{18}$$

It is obvious that the energy levels and the dispersion of the quasiparticle for $\hat{H}_{NHK}$ and $\hat{H}_0$ are the same, i.e.

$$E_{NHK}(k) \equiv \pm 2J. \tag{19}$$

This is a system with a flat band.

Here, we only discuss the case of all real eigenvalues of the non-Hermitian Hamiltonian $\hat{H}_{NHK}$. According to the quantum Liouvillian statistical theory, we obtain the Liouvillian Hamiltonian of the one-dimensional Ising model at finite temperature

$$\begin{aligned} \hat{H}_L &= -\frac{1}{\beta_T}\ln[\hat{S}(e^{-\beta_T\hat{H}_0})\hat{S}^\dagger] \\ &= \sum_{k>0}\psi_k^\dagger[\hat{h}_L(k)]\psi_k, \end{aligned} \tag{20}$$

where

$$\hat{h}_L(k) = \frac{\varepsilon_k}{\sqrt{[A_y(k)]^2 + [A_z(k)]^2}}[A_y(k)\cdot\tau^y + A_z(k)\cdot\tau^z]. \tag{21}$$

The Liouvillian energy levels are $E_\pm^L = \pm\varepsilon_k$, where

$$\begin{aligned} \varepsilon_k = -\frac{1}{\beta_T}\cosh^{-1}[&\cosh(2\beta_{NH})\cdot\cosh(2\beta_T J) \\ &+ \cos k\cdot\sinh(2\beta_{NH})\cdot\sinh(2\beta_T J)]. \end{aligned} \tag{22}$$

Therefore, we can denote the energy bands of the system by a rotor

$$\vec{N}_L(k) = \frac{1}{\sqrt{[A_x(k)]^2 + [A_y(k)]^2 + [A_z(k)]^2}}(A_x(k), A_y(k), A_z(k))$$

with

$$\begin{aligned} A_x(k) &= 0, \\ A_y(k) &= \frac{-\sin k}{\cosh(2\beta_{NH})}, \\ A_z(k) &= \cos k + \tanh(2\beta_{NH})\cdot\coth(2\beta_T J). \end{aligned} \tag{23}$$

As a result, the non-Hermitian terms lead to unexpected physics consequences: On the one hand, they change the energy dispersion from $E_{NHK}(k) = \pm 2J$ to $E_\pm^L(k) = \pm\varepsilon_k$. See the illustration in figure 1; on the other hand, they rotate the rotor of energy bands from $(0, J\sin k, -J\cos k)$ to $\frac{1}{\sqrt{[A_y(k)]^2 + [A_z(k)]^2}}(0, A_y(k), A_z(k))$. With increasing the non-Hermitian strength β_{NH}, the original flat energy bands become *dispersive*. In addition, the non-Hermitian terms change the energy gap from $\Delta = 4|J|$ to $\Delta = 4\left|\frac{\beta_{NH}}{\beta_T} \pm J\right|$.

3.2. The 'topological phase diagram' and 'pseudo-phase transition'

We use the Jordan–Wigner transformation to map the non-Hermitian Ising model to a one-dimensional Kitaev model with an imbalanced p-wave superconductor. Therefore, by studying the topological properties of the one-dimensional Kitaev model with an imbalanced p-wave superconductor, we can know the properties of the non-Hermitian Ising model.

The Liouvillian Hamiltonian $\hat{H}_L = \sum_k \psi_k^\dagger[\hat{h}_L(k)]\psi_k$ can be divided into three parts

$$\hat{H}_L = \hat{H}_{L,k>0} + \hat{H}_{L,k=0} + \hat{H}_{L,k=\pi}. \tag{24}$$

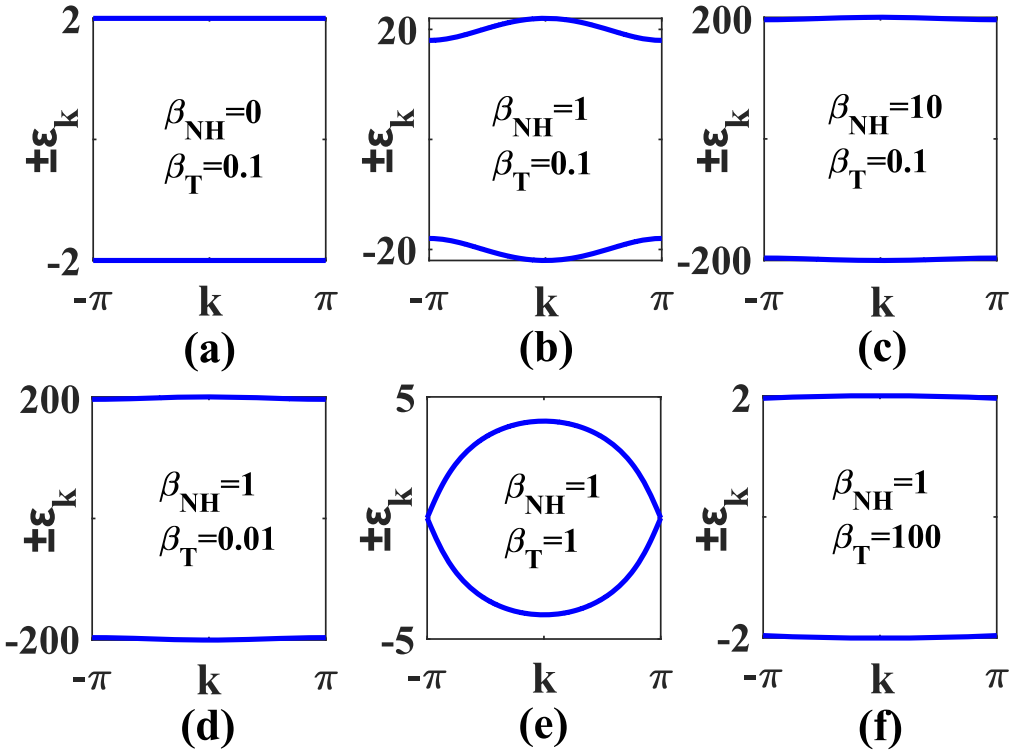

Figure 1. The Liouvillian energy levels $E_{\pm}^{L}=\pm\varepsilon_k$ of the Liouvillian Hamiltonian $\hat{H}_L$. Here, $J=1$.

After diagonalizing the fermion Hamiltonian $\hat{H}_L$ at the points $k>0$, we have

$$\hat{H}_{L,k>0}=\sum_{k>0}\varepsilon(k)\alpha_k^{\dagger}\alpha_k-\sum_{k>0}\varepsilon(k)\alpha_{-k}\alpha_{-k}^{\dagger}, \tag{25}$$

where α_k and $\alpha_k^{\dagger}$ are annihilation and creation operators of diagonalized quasiparticles and $\alpha_{\pm k}$ annihilate the ground state $|G\rangle$, i.e. $\alpha_{\pm k}|G\rangle=0$. Both α bands have positive energy at each point in momentum space $k>0$. The Hamiltonian at $k=0$ and $k=\pi$ are diagonalized into

$$\begin{aligned}\hat{H}_{L,k=0}&=\varepsilon(k=0)\alpha_{k=0}^{\dagger}\alpha_{k=0},\\ \hat{H}_{L,k=\pi}&=\varepsilon(k=\pi)\alpha_{k=\pi}^{\dagger}\alpha_{k=\pi},\end{aligned} \tag{26}$$

where $\varepsilon(k=0)=-2\left(\frac{\beta_{\rm NH}}{\beta_T}+J\right)$ and $\varepsilon(k=\pi)=-2\left(\frac{\beta_{\rm NH}}{\beta_T}-J\right)$.

To describe the 'topological' properties of $\hat{H}_L$, we define two Z_2 'topological' invariants—*Pfaffians* at high symmetry points $k=0$ and $k=\pi$ in momentum space

$$\begin{aligned}\eta_{_{k=0}}&=\langle\Psi|\ c_{k=0}^{\dagger}c_{k=0}|\Psi\rangle,\\ \eta_{_{k=\pi}}&=\langle\Psi|\ c_{k=\pi}^{\dagger}c_{k=\pi}|\Psi\rangle.\end{aligned} \tag{27}$$

$|\Psi\rangle$ denotes the 'ground state' of $\hat{H}_L$, and

$$\begin{aligned}\eta_{_{k=0}}&=\frac{\varepsilon[k=0]}{|\varepsilon[k=0]|}=\frac{-2\left(\frac{\beta_{\rm NH}}{\beta_T}+J\right)}{\left|-2\left(\frac{\beta_{\rm NH}}{\beta_T}+J\right)\right|},\\ \eta_{_{k=\pi}}&=\frac{\varepsilon[k=\pi]}{|\varepsilon[k=\pi]|}=\frac{-2\left(\frac{\beta_{\rm NH}}{\beta_T}-J\right)}{\left|-2\left(\frac{\beta_{\rm NH}}{\beta_T}-J\right)\right|}.\end{aligned} \tag{28}$$

Table 1. The two Z_2 'topological' variables of four universal classes of 'topological' orders.

$\eta_{k\,=\,0}$	-1	-1	1	1
$\eta_{k\,=\,\pi}$	-1	1	-1	1

As a result, we have

$$\begin{aligned}\eta_{_{k=0}}&=\begin{cases}+1,\ \varepsilon(k=0)>0\\ -1,\ \varepsilon(k=0)<0\end{cases},\\ \eta_{_{k=0}}&=\begin{cases}+1,\ \varepsilon(k=\pi)>0\\ -1,\ \varepsilon(k=\pi)<0\end{cases}.\end{aligned} \tag{29}$$

Table 1 shows the two Z_2 'topological' invariants of four universal classes of 'topological' orders.

When $\eta_{_{k=0}}\cdot\eta_{_{k=\pi}}=-1$ $((\eta_{_{k=0}},\eta_{_{k=\pi}})=(-1,1)$, or $(1,-1))$, we have a 'topological' phase; When $\eta_{_{k=0}}\cdot\eta_{_{k=\pi}}=1$ $((\eta_{_{k=0}},\eta_{_{k=\pi}})=(1,1)$, or $(-1,-1))$, we have a 'non-topological' phase. This is different from the case of the phase at zero temperature for the Hermitian Ising model, in which the phase of $(\eta_{_{k=0}},\eta_{_{k=\pi}})=(-1,1)$ corresponds to ferromagnetic order; the phase of $(1,-1)$ corresponds to antiferromagnetic order; the phase of $(\eta_{_{k=0}},\eta_{_{k=\pi}})=(1,1)$ corresponds to a spin-polarized phase denoted by $|\rightarrow\rightarrow\rightarrow\rightarrow\rangle$; the phase of $(\eta_{_{k=0}},\eta_{_{k=\pi}})=(-1,-1)$ corresponds to a spin-polarized phase denoted by $|\leftarrow\leftarrow\leftarrow\leftarrow\rangle$.

We plot the 'global phase diagram' of the Liouvillian Hamiltonian $\hat{H}_L$ via the non-Hermitian strength $\beta_{\rm NH}$ and the inverse temperature β_T in figure 2, of which the two 'topological' invariants $(\eta_{_{k=0}},\eta_{_{k=\pi}})$ are $(-1,1)$, $(-1,-1)$, $(1,1)$ in region I, II, III, respectively. As a result, region I is the

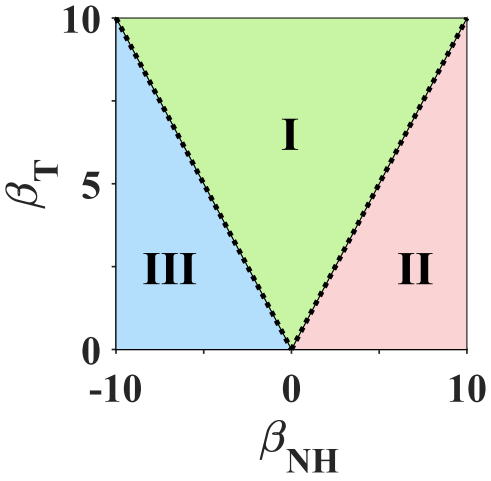

Figure 2. The 'global phase diagram' of the Liouvillian Hamiltonian $\hat{H}_L$ via the non-Hermitian strength $\beta_{\rm NH}$ and the inverse temperature β_T. The two Z_2 'topological' invariants ($\eta_{k=0}$, $\eta_{k=\pi}$) are $(-1, 1)$, $(-1, -1)$, $(1, 1)$ in region I, II, and III, respectively. The dashed line $\frac{\beta_{\rm NH}}{\beta_T} = \pm J$ denotes the 'pseudo-phase transition' between the 'topological' phase (region I) and the 'non-topological' phases (regions II and III).

'topological' phase; regions II and III are the 'non-topological' phases. The 'topological phase transition' occurs between these two phases, at which the Liouvillian energy gap is closed ($\Delta = 4\left|\frac{\beta_{\rm NH}}{\beta_T} \pm J\right| = 0$) that determines $\frac{\beta_{\rm NH}}{\beta_T} = \pm J$. Due to the nature of finite temperature, this 'topological phase transition' is a crossover. Thus, we call it '*pseudo-phase transition*' and denote it by a dashed line in figure 2.

3.3. The thermodynamic properties

According to equations (20)–(23) and using the Jordan–Wigner transformation and the Fourier transform, we can get

$$\begin{aligned}\hat{H}_L = &\frac{\varepsilon_k}{\sqrt{[A_y(k)]^2 + [A_z(k)]^2}}\sum_j\Bigg[\frac{1+\frac{1}{\cosh(2\beta_{\rm NH})}}{2}\sigma_j^x c_{j+1}^x \\ &+\frac{1-\frac{1}{\cosh(2\beta_{\rm NH})}}{2}\sigma_j^y c_{j+1}^y \\ &+\tanh(2\beta_{\rm NH})\cdot\coth(2\beta_T J)\sigma_j^z\Bigg].\end{aligned} \tag{30}$$

From this, we find the Liouvillian Hamiltonian $\hat{H}_L$ describes *an effective anisotropic XY model in a transverse field* [49–51], of which the effective transverse field is

$$h = \tanh(2\beta_{\rm NH})\cdot\coth(2J\beta_T), \tag{31}$$

and the anisotropy ratio is

$$\gamma = \frac{1}{\cosh(2\beta_{\rm NH})}. \tag{32}$$

Thus we use the effective transverse field h and the anisotropy ratio γ to show the 'global phase diagram' of the Liouvillian Hamiltonian $\hat{H}_L$ in figure 3, in which the white regions (I regions) are forbidden. Likewise, the 'pseudo-phase transition' denoted by a dashed line occurs between the 'topological' phase (II regions) and the 'non-topological' phase (III regions).

3.3.1. The Hermitian case $\beta_{NH} = 0$. For the Hermitian case $\beta_{\rm NH} = 0$, the Liouvillian Hamiltonian $\hat{H}_L$ is reduced to $\hat{H}_0$ and the results become trivial: there exists the correspondence between the ground states and the zero-temperature states, and the thermalization effect in the high-temperature limit. The system is on point 'c' in figure 3.

3.3.2. The zero temperature $\beta_T \to \infty$. For the case of $\beta_{\rm NH} \neq 0$, the system becomes non-Hermitian. Near zero temperature (or $\beta_T \to \infty$), due to $\coth(2J\beta_T) \to 1$, we have

$$h^2 + \gamma^2 \equiv 1. \tag{33}$$

As a result, $\hat{H}_L$ becomes an anisotropic XY model near zero temperature and the system is on the quarter circle (red curve in figure 3). Now, with increasing non-Hermitian strength $|\beta_{\rm NH}|$, the system shifts from $h = 0$, $\gamma = 1$ (denoted by point 'c') to point $h = 1$, $\gamma = 0$ (denoted by point 'p') in figure 3. The existence of the quarter circle in figure 3 indicates the collapse of the correspondence between the ground states and the zero-temperature states. At a fixed finite temperature, with increasing non-Hermitian strength $|\beta_{\rm NH}|$, the quarter circle becomes the quarter ellipse, as seen in the purple curve in figure 3(a).

To better reflect the characteristics of the system at zero temperature, we calculate the expected value of spin correlation which is defined as

$$\langle\sigma_i^\mu\sigma_{i+L}^\mu\rangle = \frac{{\rm Tr}\,(\sigma_i^\mu\sigma_{i+L}^\mu\cdot\rho_{\rm NHTS}^S)}{{\rm Tr}\,(\rho_{\rm NHTS}^S)}. \tag{34}$$

Because $\rho_{\rm NHTS}^S$ is not involved any term about σ_y, we have $\langle\sigma_i^y\sigma_{i+L}^y\rangle = 0$. The calculation of $\langle\sigma_i^z\sigma_{i+L}^z\rangle$ is obtained as $\langle\sigma_i^z\sigma_{i+L}^z\rangle = \tanh^2(\beta_{\rm NH})$. The spin correlation $\langle\sigma_i^x\sigma_{i+L}^x\rangle$ can be mapped to the Green function of fermions [52], i.e.

$$\langle\sigma_i^x\sigma_{i+L}^x\rangle = \begin{vmatrix} G_{i,i+1} & G_{i,i+2} & \ldots & G_{i,i+L} \\ \vdots & \ldots & \ldots & \vdots \\ G_{i+L-1,i+1} & \ldots & \ldots & G_{i+L-1,i+L}\end{vmatrix}, \tag{35}$$

where $G_{i,j}$ is defined by $G_{i,j} = \langle(c_i^\dagger - c_i)(c_j^\dagger + c_j)\rangle$. For the case of $N \to \infty$ and $i - j = r$, we have

$$\begin{aligned}G_r = &\frac{1+1/\cosh(2\beta_{\rm NH})}{2}L_{r+1} + \frac{1-1/\cosh(2\beta_{\rm NH})}{2}L_{r-1} \\ &+\tanh(2\beta_{\rm NH})\coth(2J\beta_T)L_r,\end{aligned} \tag{36}$$

where

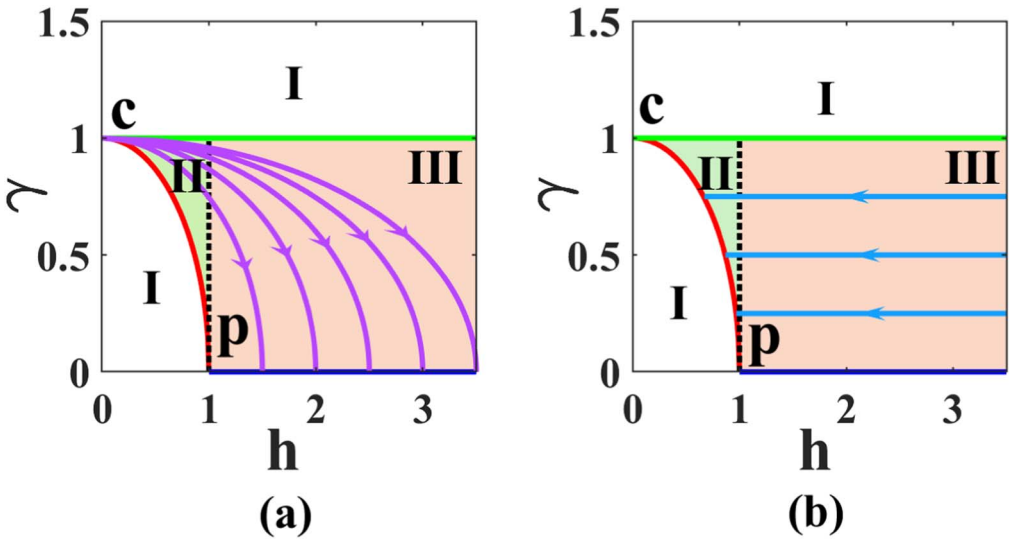

Figure 3. The 'Global phase diagram' of the Liouvillian Hamiltonian $\hat{H}_L$ via the effective transverse field $h = \tanh(2\beta_{\rm NH}) \cdot \coth(2J\beta_T)$ and the anisotropy ratio $\gamma = 1/\cosh(2\beta_{\rm NH})$. The white regions (region I) are forbidden. The dashed line denotes the 'pseudo-phase transition' between the 'topological' phase (region II) and the 'non-topological' phase (region III). (a) The flow of the system with increasing non-Hermitian strength $\beta_{\rm NH}$ at fixed temperature T. (b) The flow of the system with decreasing temperature T at fixed non-Hermitian strength $\beta_{\rm NH}$.

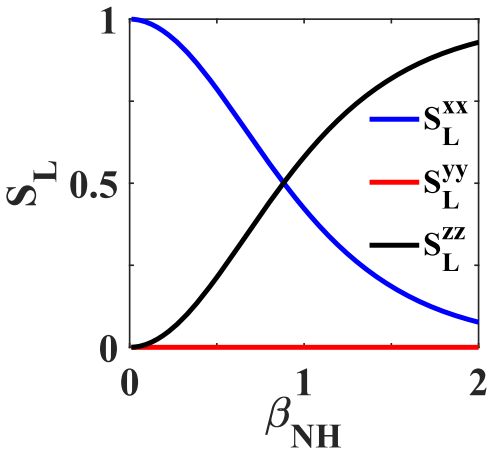

Figure 4. The spin correlations S_L^{xx}, S_L^{yy} and S_L^{zz} at low temperature $T = 0.02J$. Here, $L = 10$.

3.3.3. The strongly non-Hermitian case $\beta_{NH} \to \pm\infty$. For the case of a strong non-Hermitian strength limit, $\beta_{\rm NH} \to \pm\infty$, the original non-Hermitian Hamiltonian $\hat{H}_{\rm NHIS}$ turns into

$$-J e^{|\beta_{\rm NH}|} \sum_j \sigma_j^+ \sigma_{j+1}^+, \tag{38}$$

or

$$-J e^{|\beta_{\rm NH}|} \sum_j \sigma_j^- \sigma_{j+1}^-. \tag{39}$$

Due to $\gamma = 1/\cosh(2\beta_{\rm NH}) \to 0$, the Liouvillian Hamiltonian $\hat{H}_L$ is reduced into an effective *isotropic* XY model in the transverse field. Now, at finite temperature ($\beta_T \nrightarrow \infty$), the Liouvillian energy levels are obtained as

$$E_\pm^L \simeq \pm 2\frac{\beta_{\rm NH}}{\beta_T} \pm \frac{1}{\beta_T} \ln\left[\cosh(2J\beta_T) + \cos k \cdot \sinh(2J\beta_T)\right], \tag{40}$$

$$L_r = \frac{1}{\pi}\int_0^\pi \left(\frac{\cos(rk)\mathrm{d}k}{\sqrt{1 - \sin^2 k \cdot \tanh^2(2\beta_{\rm NH}) + 2\cos k \cdot \tanh(2\beta_{\rm NH}) \cdot \coth(2J\beta_T) + \tanh^2(2\beta_{\rm NH}) \cdot \coth^2(2J\beta_T)}} \right.$$
$$\left. \cdot \sqrt{1 - \frac{2}{\cosh(2\beta_{\rm NH}) \cdot \cosh(2J\beta_T) + \cos k \cdot \sinh(2\beta_{\rm NH}) \cdot \sinh(2J\beta_T) + 1}} \right). \tag{37}$$

We show the spin correlation S_L at the low temperature of $T = 0.02J$ in figure 4. With the increase of the non-Hermitian strength, the spin correlation function in the z-direction becomes larger, while that in the x-direction becomes smaller, indicating that all the spins of the system are shifted to the z-direction.

and the rotor of energy bands is fixed to be

$$\vec{N}(k) = (0, 0, 1). \tag{41}$$

The system is on the blue line in figure 3. With decreasing the temperature T, the system approaches the point $h = 1$, $\gamma = 0$ (denoted by point 'p' in figure 3) from $h \to \infty$, $\gamma = 0$. Near

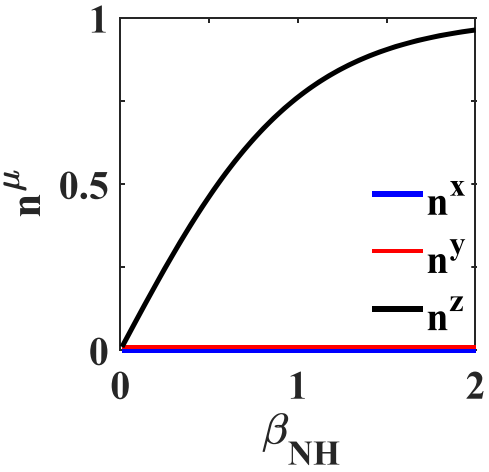

Figure 5. The expected values of local magnetizations n^μ ($\mu = x, y, z$) at high temperature $T = 20J$. Here, $L = 10$.

zero temperature with $\beta_T \to \infty$, the system trends closer to the singular point at 'p' in figure 3. Now, Liouvillian energy dispersions are reduced into

$$E_\pm^L \simeq \pm\frac{2}{\beta_T}(\beta_{\rm NH} + J\beta_T), \tag{42}$$

for $k \sim \pi$ or

$$E_\pm^L \simeq \pm\frac{2}{\beta_T}(\beta_{\rm NH} - J\beta_T), \tag{43}$$

for $k \sim \pi$. We have an effective 'Liouvillian Hamiltonian' $\hat{H}_{\rm L}' \sim -2\hat{H}'$ for $k \sim \pi$ at the effective 'temperature' $T_{\rm eff} = \frac{1}{k_{\rm B}(\beta_{\rm NH} + J\beta_T)}$ or $\hat{H}_L' \sim -2\hat{H}'$ for $k \sim \pi$ at effective 'temperature' $T_{\rm eff} = \frac{1}{k_{\rm B}(\beta_{\rm NH} - J\beta_T)}$. Nevertheless, at a given finite non-Hermitian strength, with decreasing the temperature T, the system is at the dodger blue line in figure 3(b).

3.3.4. The high-temperature case $\beta_T \to 0$. In the high-temperature limit of $\beta_T \to 0$, we have a temperature-dependent Hamiltonian $\hat{H}_{\rm L} \sim -\frac{2}{\beta_T}\hat{H}'$ at temperature T or a pseudo-temperature–independent pseudo-Hamiltonian $\hat{H}_{\rm eff}^{\rm pseudo} = -2\hat{H}'$ at pseudo-temperature $T^{\rm pseudo} = 1/\beta_{\rm NH}$. The situation is very different from that of the usual Hermitian model, in which there exists the thermalization effect in the high-temperature limit ($T \to \infty$) due to $e^{-\beta_T \hat{H}_0} \sim 1$ and the correspondence between the ground states and the zero-temperature states. In addition, as $\beta_T \to 0$ and $|\beta_{\rm NH}| \to \infty$, the 'ground state' of $\hat{H}_{\rm eff}^{\rm pseudo}$ describes a 'non-topological' state (regions II, III in figure 2).

To better see this phenomenon, we show the expected values of local magnetizations

$$n^\mu = \frac{1}{N}\sum_i \langle\sigma_i^\mu\rangle, \tag{44}$$

where the expected values of the spin operators σ_i^μ ($\mu = x, y, z$) are

$$\langle\sigma_i^\mu\rangle = \frac{{\rm Tr}\,(\sigma_i^\mu \cdot \rho_{\rm NHTS}^S)}{{\rm Tr}\,(\rho_{\rm NHTS}^S)}, \tag{45}$$

and N is the number of lattice sites in figure 5. After calculation, we have

$$\begin{aligned} n^x &= 0, \\ n^y &= 0, \\ n^z &= \tanh(\beta_{\rm NH}), \end{aligned} \tag{46}$$

for the system at the high temperature $T = 20J$. This result ($n^z \neq 0$ if $\beta_{\rm NH} \neq 0$) clearly indicates *the non-thermalization effect in the high-temperature limit*.

4. Conclusions

In the paper, we study the one-dimensional non-Hermitian Ising model at finite temperature with the help of the quantum Liouvillian statistical theory. A 'pseudo-phase transition' is discovered between the 'topological' phase and the 'non-topological' phase. Compared with the usual energy gap closed in the Hermitian system, the 'pseudo-phase transition' is accompanied by the Liouvillian energy gap closed. Moreover, we show that its Liouvillian Hamiltonian $\hat{H}_{\rm L}$ can be reduced to an effective anisotropic XY model in the transverse field. In the Hermitian case, the system shows the thermalization in the high-temperature limit and the correspondence between the ground states and the zero-temperature states. Near the zero temperature, we find that all spins of the system are shifted to one direction (z-direction). For the case of a strong non-Hermitian strength limit, the system becomes an effective isotropic XY model in the transverse field. In the high-temperature limit, the system appears the non-thermalization. This work will promote the study of the physical properties of non-Hermitian systems at finite temperatures.

Acknowledgments

This work is supported by NSFC Grant No. 11 974 053, 12 174 030.

References

[1] De Cipra B A 1987 An introduction to the Ising model *Am. Math. Monthly* **94** 937
[2] Binder K 1981 Finite size scaling analysis of ising model block distribution functions Z *Phys. B Condens. Matter* **43** 119
[3] Newell G F and Montroll E W 1953 On the theory of the Ising model of ferromagnetism *Rev. Mod. Phys.* **25** 353
[4] Pfeuty P 1970 The one-dimensional Ising model with a transverse field *Ann. Phys.* **57** 79
[5] Elliott R J and Wood C 1971 The Ising model with a transverse field. I. High temperature expansion *J. Phys. C: Solid St. Phys.* **4** 2359
[6] Pfeuty P and Elliott R J 1971 The Ising model with a transverse field. II. Ground state properties *J. Phys. C: Solid St. Phys.* **4** 2370
[7] Stinchcombe R B 1973 Ising model in a transverse field. I. Basic theory *J. Phys. C: Solid St. Phys.* **6** 2459

[8] Elliott R J, Pfeuty P and Wood C 1970 Ising model with a transverse field *Phys. Rev. Lett.* **25** 443

[9] Sachdev S 1999 *Quantum Phase Transitions* (Cambridge, UK: Cambridge University Press)

[10] Carr L D 2010 *Understanding Quantum Phase Transitions* (Boca Raton: CRC Press)

[11] Suzuki S, Inoue J and Chakrabarti B K 2012 *Quantum Ising Phases and Transitions in Transverse Ising Models* (Heidelberg: Springer)

[12] Heyl M, Polkovnikov A and Kehrein S 2013 Dynamical quantum phase transitions in the transverse-field ising model *Phys. Rev. Lett.* **110** 135704

[13] Bender C M 2007 Making sense of non-Hermitian Hamiltonians *Rep. Prog. Phys.* **70** 947

[14] Ashida Y, Gong Z and Ueda M 2020 Non-hermitian physics *Adv. Phys.* **69** 249

[15] Brody D C 2014 Biorthogonal quantum mechanics *J. Phys. A: Math. Theor.* **47** 035305

[16] Heiss W D 2004 Exceptional points of non-Hermitian operators *J. Phys. A: Math. Theor.* **37** 2455–67

[17] Heiss W D 2012 The physics of exceptional points *J. Phys. A: Math. Theor.* **45** 444016

[18] Bender C M 1998 Real spectra in non-Hermitian Hamiltonians having PT-symmetry *Phys. Rev. Lett.* **80** 5243–6

[19] Bender C M, Brody D C and Jones H F 2002 Complex extension of quantum mechanics *Phys. Rev. Lett.* **89** 270401

[20] Ahmed Z 2002 Pseudo-hermiticity of hamiltonians under gauge-like transformation: real spectrum of non-hermitian hamiltonians *Phys. Lett.* A **294** 287–91

[21] Mostafazadeh A 2002 Pseudo-Hermiticity versus PT symmetry: The necessary condition for the reality of the spectrum of a non-Hermitian Hamiltonian *J. Math. Phys.* **43** 205

Mostafazadeh A 2002 Pseudo-Hermiticity versus PT-symmetry. II. A complete characterization of non-Hermitian Hamiltonians with a real spectrum *J. Math. Phys.* **43** 2814

Mostafazadeh A 2002 Pseudo-Hermiticity versus PT-symmetry III: Equivalence of pseudo-Hermiticity and the presence of antilinear symmetries *J. Math. Phys.* **43** 3944

[22] Rüer C E, Makris K G, El-Ganainy R, Christodoulides D N, Segev M and Kip D 2010 Observation of parity-time symmetry in optics *Nat. Phys.* **6** 192

[23] Hang C, Huang G and Konotop V V 2013 PT-symmetry with a system of three-Level atoms *Phys. Rev. Lett.* **110** 083604

[24] Peng P, Cao1 W, Shen C, Qu W, Wen J, Jiang L and Xiao Y 2016 Anti-parity-time symmetry with flying atoms *Nat. Phys.* **12** 1139–45

[25] Zhang Z, Zhang Z, Zhang Y, Sheng J, Yang L, Miri M-A, Christodoulides D N, He B, Zhang Y and Xiao M 2016 Observation of Parity-Time symmetry in optically induced atomic lattices *Phys. Rev. Lett.* **117** 123601

[26] Bender N, Factor S, Bodyfelt J D, Ramezani H, Christodoulides D N, Ellis F M and Kottos T 2013 Observation of asymmetric transport in structures with active nonlinearities *Phys. Rev. Lett.* **110** 234101

[27] Assawaworrarit S, Yu X and Fan S 2017 Robust wireless power transfer using a nonlinear parity-time-symmetric circuit *Nature* **546** 387

[28] Choi Y, Hahn C, Yoon J W and Song S H 2018 Observation of an anti-PT-symmetric exceptional point and energy-difference conserving dynamics in electrical circuit resonators *Nat. Commun.* **9** 2182

[29] Bittner S, Dietz B, G¨ther U, Harney H L, Miski-Oglu M, Richter A and Schfer F 2012 PT-symmetry and spontaneous symmetry breaking in a microwave billiard *Phys. Rev. Lett.* **108** 024101

[30] Zhu X, Ramezani H, Shi C, Zhu J and Zhang X 2014 PT-symmetric acoustics *Phys. Rev.* X **4** 031042

[31] Popa B-I and Cummer S A 2014 Non-reciprocal and highly nonlinear active acoustic metamaterials *Nat. Commun.* **5** 3398

[32] Fleury R, Sounas D and Alù A 2015 An invisible acoustic sensor based on parity-time symmetry *Nat. Commun.* **6** 5905

[33] Wu Y, Liu W, Geng J, Song X, Ye X, Duan C-K, Rong X and Du J 2019 Observation of parity-time symmetry breaking in a single-spin system *Science* **364** 878

[34] Kunst F K, Edvardsson E, Budich J C and Bergholtz E J 2018 Biorthogonal bulk-boundary correspondence in non-Hermitian systems *Phys. Rev. Lett.* **121** 026808

[35] Yokomizo K and Murakami S 2019 Non-Bloch band theory of non-Hermitian systems *Phys. Rev. Lett.* **123** 066404

[36] Xiao L, Deng T, Wang K, Zhu G, Wang Z, Yi W and Xue P 2020 Non-Hermitian bulk¨Cboundary correspondence in quantum dynamics *Nat. Phys.* **16** 761–6

[37] Yang Z, Zhang K, Fang C and Hu J 2020 Non-Hermitian bulk-boundary correspondence and auxiliary generalized Brillouin zone theory *Phys. Rev. Lett.* **125** 226402

[38] Xiong Y 2018 Why does bulk boundary correspondence fail in some non-hermitian topological models *J. Phys. Commun.* **2** 035043

[39] Yao S, Song F and Wang Z 2018 Non-hermitian chern bands *Phys. Rev. Lett.* **121** 136802

[40] Wang X-R, Guo C-X and Kou S-P 2020 Defective edge states and number-anomalous bulk-boundary correspondence in non-Hermitian topological systems *Phys. Rev.* B **101** 121116(R)

[41] Yao S and Wang Z 2018 Edge states and topological invariants of non-hermitian systems *Phys. Rev. Lett.* **121** 086803

[42] Song F, Yao S and Wang Z 2019 Non-Hermitian skin effect and chiral damping in open quantum systems *Phys. Rev. Lett.* **123** 170401

[43] Okuma N, Kawabata K, Shiozaki K and Sato M 2020 Topological origin of non-Hermitian skin effects *Phys. Rev. Lett.* **124** 086801

[44] Du Q, Cao K and Kou S-P 2022 Physics of PT-symmetric quantum systems at finite temperatures *Phys. Rev.* A **106** 032206

[45] Deguchi T and Ghosh P K 2009 The exactly solvable quasi-Hermitian transverse Ising model *J. Phys.* A **42** 475208

[46] Kitaev A Y 2001 Unpaired Majorana fermions in quantum wires *Phys. Usp.* **44** 131

[47] Li C, Zhang X Z, Zhang G and Song Z 2018 Topological phases in a Kitaev chain with imbalanced pairing *Phys. Rev.* B **97** 115436

[48] Zhao X-M, Guo C-X, Yang M-L, Wang H, Liu W-M and Kou S-P 2021 Anomalous non-Abelian statistics for non-Hermitian generalization of Majorana zero modes *Phys. Rev.* B **104** 214502

[49] Bunder J E and McKenzie R H 1999 Effect of disorder on quantum phase transitions in anisotropic XY spin chains in a transverse field *Phys. Rev.* B **60** 344

[50] Campbell S, Richens J, Gullo N L and Busch T 2013 Criticality, factorization, and long-range correlations in the anisotropic XY model *Phys. Rev.* A **88** 062305

[51] Luo Q, Zhao J and Wang X 2018 Fidelity susceptibility of the anisotropic XY model: The exact solution *Phys. Rev.* A **98** 022106

[52] Lieb E, Schultz T and Mattis D 1961 Two soluble models of an antiferromagnetic chain *Ann. Phys.* **16** 407